APPROPRIATE LINE PROFILES FOR RADIATION MODELING IN THE DETECTION OF ATMOSPHERIC POLLUTANTS

A Technical Report
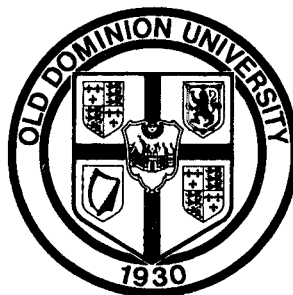
By

Prepared for the

NATIONAL AERONAUTICS AND SPACE ADMINISTRATION
LANGLEY RESEARCH CENTER
HAMPTON, VIRGINIA 23365

Under
Master Contract Agreement NAS1-9434
Task Order No. 53

SCHOOL OF ENGINEERING
OLD DOMINION UNIVERSITY
NORFOLK, VIRGINIA

NASA CR- 132303

NAS1-9434-53

APPROPRIATE LINE PROFILES FOR RADIATION MODELING IN THE DETECTION OF ATMOSPHERIC POLLUTANTS

A TECHNICAL REPORT

By
Surendra N. Tiwari
Associate Professor
School of Engineering
Old Dominion University

Prepared for the
NATIONAL AERONAUTICS AND SPACE ADMINISTRATION
Langley Research Center
Hampton, Virginia 23365

Under
Master Contract Agreement No. NAS1-9434
Task Order No. 53

Submitted by the
Old Dominion University Research Foundation
P.O. Box 6173
Norfolk, Virginia 23508

March 1973

FOREWORD

This is a report on Radiation Modeling in the Detection of
Atmospheric Pollutants. The work was done at the NASA-Langley
Research Center, during the Summer and Fall of 1972, under the
Contract No. NAS1-9434-53. The contract was monitored by
Dr. Henry G. Reichle.

CONTENTS

APPROPRIATE LINE PROFILES FOR RADIATION MODELING

IN THE DETECTION OF ATMOSPHERIC POLLUTANTS

by Surendra N. Tiwari

Thermal Engineering Department

Old Dominion University, Norfolk, Virginia 23508

SUMMARY

Absorption by Lorentz, Doppler, and Voight lines are compared
for a range of atmospheric parameters. It is found that, for the
intermediate path lengths, the use of the combined Lorentz-Doppler
(Voight) profile is essential in calculating the atmospheric trans-
mittance. A brief review of band models, to approximate the absorption
over certain frequency interval, is presented. Expressions for total
radiative energy emergent from the atmosphere are given which, with
appropriate line or band models, can be used to reduce the data obtained
from radiation measurement by an instrument mounted on an aircraft or
a satellite. By employing the inversion procedure, the concentration
of atmospheric pollutants can be obtained from the measured data.

I. INTRODUCTION

The study of infrared radiative transmission in actual atmospheres requires a detailed knowledge of the atmospheric constituents which absorb and emit significantly in the infrared. Specifically this means identification of infrared band of major constituents and evaluation of the line parameters of these bands. The line parameters depend upon the temperature, pressure, and concentration of the absorbing molecules and, in general, these quantities vary continuously along a nonhomogeneous path through the atmosphere.

With the availability of high resolution spectrometers, it is now possible to determine the line positions, intensities, and half widths of spectral lines of major atmospheric constituents quite accurately [1-3]. Once these fundamental molecular properties are known then it simply becomes a matter of employing either a suitable line or band model to evaluate the spectral absorption coefficient and subsequently find the atmospheric transmittance.

Because of the complexity of the vibration-rotation spectrum, the radiative transmittance is usually calculated by employing the molecular band models for homogeneous atmosphere. Through certain scaling approximation, such as Curtis-Godson approximation, the solution is then extended to the case of nonhomogeneous atmosphere. It should be realized, however, that most band models are nothing but interpolation formulas which at best correlate the laboratory measured data simulated under homogeneous conditions. Consequently these models have limited range of applicability in pressure, temperature and absorber thickness. While band

models are very useful in treating radiative transfer problems arising in the various areas of gas dynamics [4,5], their validity is restricted for actual atmospheric applications [6].

The purpose of the present paper is to investigate the feasibility of appropriate line profiles for radiation modeling in the detection of atmospheric pollutants. Discussions regarding appropriate line profiles are presented in Section II. In Section III, integrated absorptions by individual lines are calculated by employing the Lorentz, Doppler, and combined Lorentz-Doppler (Voight) profiles, and various results are compared for a range of atmospheric parameters. A review of different band models and band absorptance correlations is presented in Section IV, and expressions for upwelling atmospheric radiation are given in Section V.

The present formulation is based on the assumption of homogeneous atmosphere. However, by dividing the atmosphere in appropriate number of isothermal layers, the analyses could be extended to the case of non-homogeneous atmosphere.

II. SPECTRAL LINE PROFILE

In order to describe the infrared absorption characteristics of a radiating molecule it is necessary to consider the variation of the spectral absorption coefficient for a single line. In general, for a single line centered at the wave number ω_j, this is expressed as

$$\kappa_{\omega j} = S_j \, f_j(\omega, \gamma_j) \, , \tag{2.1}$$

where S_j is the intensity of the jth spectral line and is given by

$$S_j = \int_{-\infty}^{\infty} \kappa_{\omega j} \, d(\omega - \omega_j) \, . \tag{2.2}$$

The line intensity may be described in terms of the molecular number density and Einstein coefficients, i.e., it depends upon the transition probabilities between the initial and final states and upon the populations of these states. For a perfect gas it may be shown that S_j is a function solely of temperature. The quantity $f_j(\omega, \gamma_j)$ is the line shape factor for the jth spectral line. It is a function of the wave number ω and the line half width γ_j and is normalized on $(\omega - \omega_j)$ such that

$$\int_{-\infty}^{\infty} f_j(\omega - \omega_j) \, d(\omega - \omega_j) = 1 \, . \tag{2.3}$$

Several approximate line profiles have been described in the literature. Most commonly used profiles are rectangular, triangular, Lorentz, Doppler, or Voight (combined Lorentz and Doppler) profiles. Lorentz, Doppler, and Voight profiles are of special interest in the atmospheric studies.

The line profile usually employed for studies of infrared radiative transfer in the earth's atmosphere is the Lorentz pressure broadened line shape for which the shape factor is given by

$$f(\omega, \omega_j, \gamma_L) = \gamma_L / \{\pi[(\omega-\omega_j)^2 + \gamma_L^2]\} , \qquad (2.4)$$

where γ_L is the Lorentz half-width of the jth spectral line, (i.e., half the total line-width at half-intensity). Variation of the spectral absorption coefficient for the Lorentz lines may now be expressed as

$$\kappa_{\omega j} = S_j \gamma_L / \{\pi[(\omega - \omega_j)^2 + \gamma_L^2]\} . \qquad (2.5)$$

From simple kinetic theory, the Lorentz line half-width may be shown to vary with pressure and temperature as

$$\gamma_L \sim (P/\sqrt{T}) , \qquad (2.6)$$

where P is the effective pressure and T is the absolute temperature. Atmospheric gases which can absorb in the visible and infrared regions have relatively small concentrations. Thus, the pressure and the effective pressure are not significantly different.

More detailed quantum mechanical calculations also confirm the linear dependency of γ_L upon pressure, but indicate that the inverse square-root variation with temperature is often true only in the wing regions (large values of j) of vibration-rotation bands. Considering CO_2 as an example, Yamamoto et al. [7] have shown that the temperature dependency of the Lorentz line half-width may be described by $\gamma_j \sim T^{-n_j}$, and that n_j approaches 0.75 for small j, decreases with increasing j to approximately 0.3, and then increases with a further increase in j to

the kinetic theory value of 0.5. Ely and McCubbin [8] and Tubbs and Williams [9] have shown that a more appropriate value for n_j is unity for the lines in the immediate vicinity of the band center.

For Doppler broadened lines, the shape factor is given by the expression [10]

$$f(\omega, \omega_j, \gamma_D) = (1/\gamma_D) (\ln 2/\pi)^{1/2} \exp[-(\omega-\omega_j)^2 (\ln2/\gamma_D^2)] , \quad (2.7)$$

where γ_D is the Doppler half-width and is given by

$$\gamma_D = (\omega_j/c) (2 k T \ln 2/m)^{1/2} , \quad (2.8)$$

where c is the speed of light, k is the Boltzmann's constant, and m is the molecular mass.

Doppler broadening is associated with the thermal motion of molecules. From Eq. (2.8) it is clear that the Doppler width depends not only on temperature but also on molecular mass and the location of the line center. For certain atmospheric conditions, therefore, the Doppler and Lorentz widths may become equally important for a particular molecule radiating at a specific frequency. For comparable intensities and half-widths, however, the Doppler line has more absorption near the center and less in the wings than the Lorentz line (Fig. 1).

For radiative transfer analyses involving gases at low pressures (upper atmospheric conditions) it becomes imperative to incorporate the combined influence of the Lorentz and the Doppler broadening. The shape factor for the combined profile is given by [10,11]

$$f(a,v) = (a/\pi\gamma_D)(\ln 2/\pi)^{1/2} \int_{-\infty}^{\infty} \{\exp(-t^2)/[a^2 + (v-t)^2]\}dt , \quad (2.9)$$

where
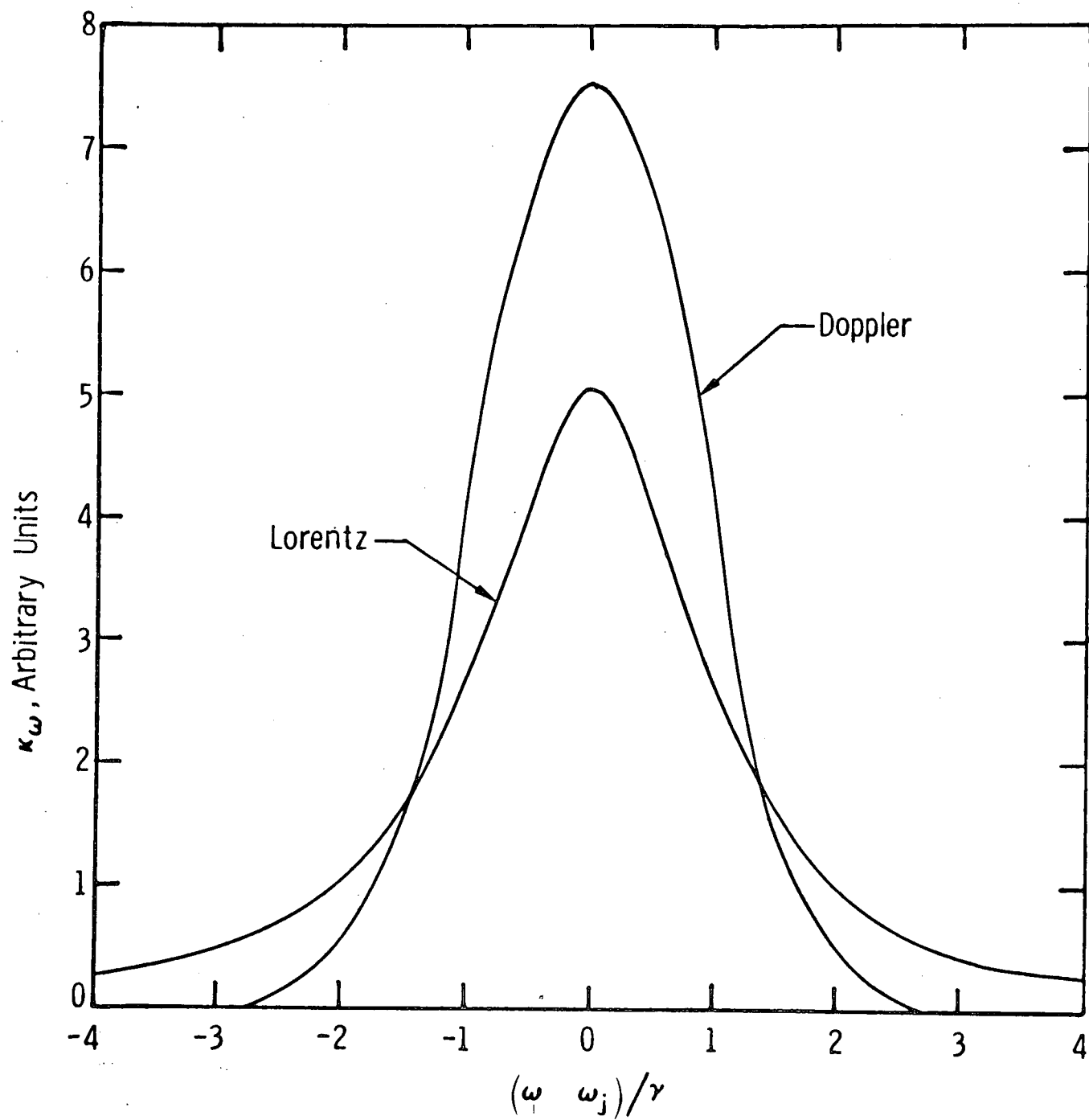
$$a = (\gamma_L/\gamma_D) (\ln 2)^{1/2} , \quad (2.10)$$

Fig. 1.   Comparison of Lorentz and Doppler line profiles

having equal line intensities

and
$$v = [(\omega - \omega_j)/\gamma_D](\ell n\ 2)^{1/2} = (\omega - \omega_j)(a/\gamma_L). \qquad (2.11)$$

Physically, a represents the ratio of Lorentz to Doppler width and v

is the wave number scaling factor.

The appropriate absorption coefficient for the combined profile

is obtained from Eq. (2.1) and (2.9) as

$$\kappa_{\omega j} = \kappa_o(\frac{a}{\pi}) \int_{-\infty}^{\infty} \{\exp(-t^2)/[a^2 + (v-t)^2]\}dt) = \kappa_o K(a,v), \qquad (2.12)$$

where

$$\kappa_o = (S_j/\gamma_D)(\ell n2/\pi)^{1/2} = (S_j/\sqrt{\pi})(a/\gamma_L) . \qquad (2.13)$$

The function K(a,v) defined in Eq. (2.12) is called the Voight function

and the line profile expressed by Eq. (2.9) is called the Voight profile.

Equation (2.12) can be expressed in the alternate form, derived

initially by Reiche [12], as

$$\kappa_{\omega j}/\kappa_o = K(a,v) = (1/\sqrt{\pi})\int_{o}^{\infty} \exp[-at - (t^2/4)] \cos(vt)\ dt . \qquad (2.14)$$

By expanding the integral in (2.14) in a Taylor series, Plass and Fivel

[13] derived a general expression for K(a,v) in powers of a as

$$K(a,v) = [\exp(a^2-v^2)\ \cos(2va)-(2/\sqrt{\pi})\sum_{n=1}^{\infty}(n!)^{-1}F^{(n)}(v)a^n\sin(n\pi/2)], \qquad (2.15)$$

where $F^{(n)}(v)$ is the nth derivative of the function

$$F(v) = \int_{o}^{\infty}\exp(-t^2)\ \sin(2vt)\ dt = \exp(-v^2)\int_{o}^{v}\exp(t^2)\ dt . \qquad (2.16)$$

For $|\omega - \omega_j| \gg \gamma_L$ and $|\omega - \omega_j| \gg \gamma_D$ Eq. (2.15) reduces to an

asymptotic form as

$$K(a,v) = (a/v^2\sqrt{\pi})[1 + (\frac{3}{2} - a^2)\frac{1}{v^2} + (\frac{15}{4} - 5a^2 + a^4)\frac{1}{v^4} + ---] . \qquad (2.17)$$

For $(v/a) \gg 1$, Born [14] has given an asymptotic expansion for $K(a,v)$ as

$$K(a,v) = \{a/[(a^2 + v^2) \sqrt{\pi}]\}[1 + (3/2\, v^2)] \ . \qquad (2.18)$$

For small values of the parameter a , Eq. (2.15) may be expressed by [15]

$$K(a,v) = \exp(-v^2)-(2a/\sqrt{\pi})[1-2vF(v)] + a^2(1-2v^2)\exp(-v^2)$$

$$- (2a^3/\sqrt{\pi})[\frac{2}{3}(1-v^2) - 2v(1 - \frac{2}{3}v^2)F(v)]$$

$$+ a^4(\frac{1}{2} - 2v^2 + \frac{2}{3}v^4)\exp(-v^2) \ . \qquad (2.19)$$

By combining Eqs. (2.1) and (2.7), the absorption coefficient for the Doppler broadened lines may now be expressed as

$$\kappa_{\omega j} = \kappa_o \exp(-v^2) \ . \qquad (2.20)$$

It should be noted that as the pressure becomes small, γ_L approaches zero and Eq. (2.12) reduces to Eq. (2.20). On the other hand, for large pressures, the quantity (γ_L/γ_D) becomes large and Eq. (2.12) reduces to the Lorentzian case, Eq. (2.5). In other words, the Voight profile assumes the Lorentzian shape in the limit of large v and reduces to the Doppler profile for small a .

Extensive reviews of the literature on the Voight function and some accurate approximations to the Voight profile are given in [10, 11, 16-18]. Armstrong [17] has presented a review of the mathematical properties of the Voight function and has discussed the various computational methods which make efficient and economical use of computer time and storage. With the aid of computer programs developed by Armstrong [17], Young [18, 19] or Hummer [20, 21], it is now possible to

calculate the Voight function, for an extended range of parameters, to an accuracy of better than six significant figures.

A simple closed form approximation to the Voight profile that is valid over a useful range of parameters is given, in terms of the present nomenclature, by [22-24]

$$\kappa_{\omega j}/\kappa_{\omega o} = [1 - (\gamma_L/\gamma_V)] \exp\{- 11.088[(\omega-\omega_j)/\gamma_V]^2\}$$

$$+ (\gamma_L/\gamma_V)/\{1 + 16 [(\omega-\omega_j)/\gamma_V]^2\} , \qquad (2.21)$$

where Voight half-width is expressed in terms of γ_L and γ_D as

$$\gamma_V = (\gamma_L/2) + [(\gamma_L^2/4) + \gamma_D^2]^{1/2} , \qquad (2.22)$$

and

$$\kappa_{\omega o} = S_j/\{\gamma_V[1.065 + 0.447(\gamma_L/\gamma_V) + 0.058(\gamma_L/\gamma_V)^2]\} . \qquad (2.23)$$

This form is very convenient for numerical computation and it matches the Voight profile within 5 per cent under worst conditions. Generally the error is within 3 per cent, with maximum errors occurring near zero pressures.

III. ABSORPTION BY INDIVIDUAL LINES

The radiative transmittance at a single wave number may, in general, be expressed as

$$\tau_\omega = \exp\left(- \int_0^X S \ f \ dX\right) , \qquad (3.1)$$

where X is the mass of the absorbing gas per unit area and is equal to the density times the thickness of the absorbing layer. For a nonhomogeneous atmosphere, X is given by the relation

$$X = \int_0^\ell \rho_a \ d\ell \qquad (3.2)$$

where ℓ is the length measured along the direction of the path which makes angle θ with the vertical, and ρ_a is the density of the absorbing gas. For a homogeneous path, Eq. (3.1) reduces to

$$\tau_{\omega j} = \exp(-S_j \ f \ X) = \exp(-\kappa_{\omega j} \ X) . \qquad (3.3)$$

For n independent lines within the wave number range of interest, the absorption coefficient is given by

$$\kappa_\omega = \sum_{j=1}^{n} \kappa_{\omega j} , \qquad (3.4)$$

and consequently the transmittance is expressed as

$$\tau = \prod_{j=1}^{n} \tau_{\omega j} . \qquad (3.5)$$

The total (integrated) absorption for a single line is given by

$$A_j = \int_{-\infty}^{\infty} (1 - \tau_{\omega j}) \ d(\omega - \omega_j) , \qquad (3.6)$$

where again ω_j represents the wave number at the line center of the jth spectral line. In astronomical and meteorological literature, the relation given by Eq. (3.6) is usually referred to as the equivalent

width of a single line.

1. Single Line with Lorentz Shape

For homogeneous atmospheric path, the absorption of an isolated spectral line of Lorentz shape, A_L, may be obtained by combining Eqs. (2.5), (3.3) and (3.6) as

$$A_L = \int_{-\infty}^{\infty} \{1-\exp(-S_j \gamma_L X/\pi[(\omega-\omega_j)^2 + \gamma_L^2])\} \, d(\omega-\omega_j) \; . \qquad (3.7)$$

In this equation, the extension of the limits to infinity is physically realistic since the absorption beyond a certain wave number from the line center is zero. By defining nondimensional quantities

$$x = S_j X/2\pi\gamma_L \; , \qquad (3.8a)$$

$$y = (\omega-\omega_j)/\gamma_L \; , \qquad (3.8b)$$

Eq. (3.7) can be written as

$$A_L = 2\gamma_L \int_{0}^{\infty} \{1 - \exp[-2x/(y^2 + 1)]\} dy \; . \qquad (3.9)$$

An exact solution of this equation is found in terms of the Landenberg-Reiche function, $L(x)$, as [25, 26]

$$A_L = 2\pi\gamma_L L(x) = 2\pi\gamma_L\{x \exp(-x)[I_0(x) + I_1(x)]\} \; , \qquad (3.10)$$

where I_0 and I_1 are the Bessel functions of imaginary arguments. Some values of the function $L(x)$ are tabulated in references [10,27]. By multiplying Eq. (2.5) by the mass of the absorbing gas, X, it can be shown that the quantity x represents one-half the optical path at the line center.

Equation (3.9) possesses two well known asymptotic forms. For small x, expanding the exponential in Eq. (3.9) in series and retaining

only the first two terms, results in

$$A_L = 4 \gamma_L x \int_0^\infty (y^2 + 1)^{-1} dy = 2\pi\gamma_L x = S_j X \, . \tag{3.11}$$

This is called the linear limit or weak line approximation. A line is called weak when $\kappa_\omega X \ll 1$ for all frequencies within the line. In this limit, absorption is independent of the pressure and is a linear function of the amount of the absorbing gas and the line intensity. According to Plass [28,29], this approximation is accurate within p per cent if $x \leq 0.02p$.

For large values of x, Eq. (3.9) reduces to

$$A_L = 2\gamma_L \int_0^\infty [1 - \exp(-2x/y^2)] \, dy \, , \tag{3.12}$$

which may be expressed in an alternate form as

$$A_L = 2\gamma_L (2x)^{1/2} \int_0^\infty \{[1 - \exp(-z^2)]/z^2\} dz \, , \tag{3.13}$$

where $z^2 = 2x/y^2$. Integration of Eq. (3.13) yields

$$A_L = 2\gamma_L (2\pi x)^{1/2} = 2(S_j \gamma_L X)^{1/2} \, . \tag{3.14}$$

This is the square-root limit or the strong line approximation and is accurate within p per cent if $x \geq (12.5/p)$. Since the line width varies linearly with the pressure, absorption in this limit varies as the square root of both the pressure and the amount of the absorbing medium. Almost all incident radiation, in this limit, is absorbed at frequencies within the total half width of the line center.

Equations (3.11) and (3.14) can also be obtained from Eq. (3.10) by expanding the modified Bessel functions for small and large values of the argument respectively [26,27]. For an extensive physical explanation of the weak and strong line approximations, see Penner [10] and

Goody [27]. The solution expressed by Eq. (3.10) is illustrated in Figure 2 along with the limiting solutions.

Three approximate relations for Eq. (3-9) are suggested in references [30,31] as

$$A_L = (2\pi\gamma_L)(2x/\pi)^{1/2}\{1 - \exp[-(\pi x/2)^{1/2}]\} \, , \qquad (3.15a)$$

$$A_L = (2\pi\gamma_L)(2x/\pi)^{1/2}[1 - \exp(-\pi x/2)]^{1/2} \, , \qquad (3.15b)$$

$$A_L = (2\pi\gamma_L)/[1 + (\pi x/2)]^{1/2} \, . \qquad (3.15c)$$

Equations (3.15) reduce to the correct asymptotic limits, and their solutions agree well with the exact solution, Eq. (3.10), over the entire range of x . Results of Eq. (3.15c) are also illustrated in Figure 2.

2. Single Line with Doppler Profile

Doppler broadening becomes important under upper atmospheric conditions. The absorption of a Doppler broadened line, A_D, is obtained by combining Eqs. (2.20), (3.3), and (3.6) as

$$A_D = [\gamma_D/(\ln 2)^{1/2}] \int_{-\infty}^{\infty}\{1 - \exp[-x_D \exp(-v^2)]\}dv \, , \qquad (3.16)$$

where $\qquad x_D = \kappa_o X = [(S_j/\gamma_D)(\ln 2/\pi)^{1/2}] X \qquad (3.17)$

represents the optical path at the line center. By expanding the exponential in an infinite series, Eq. (3.16) can be written as [10]

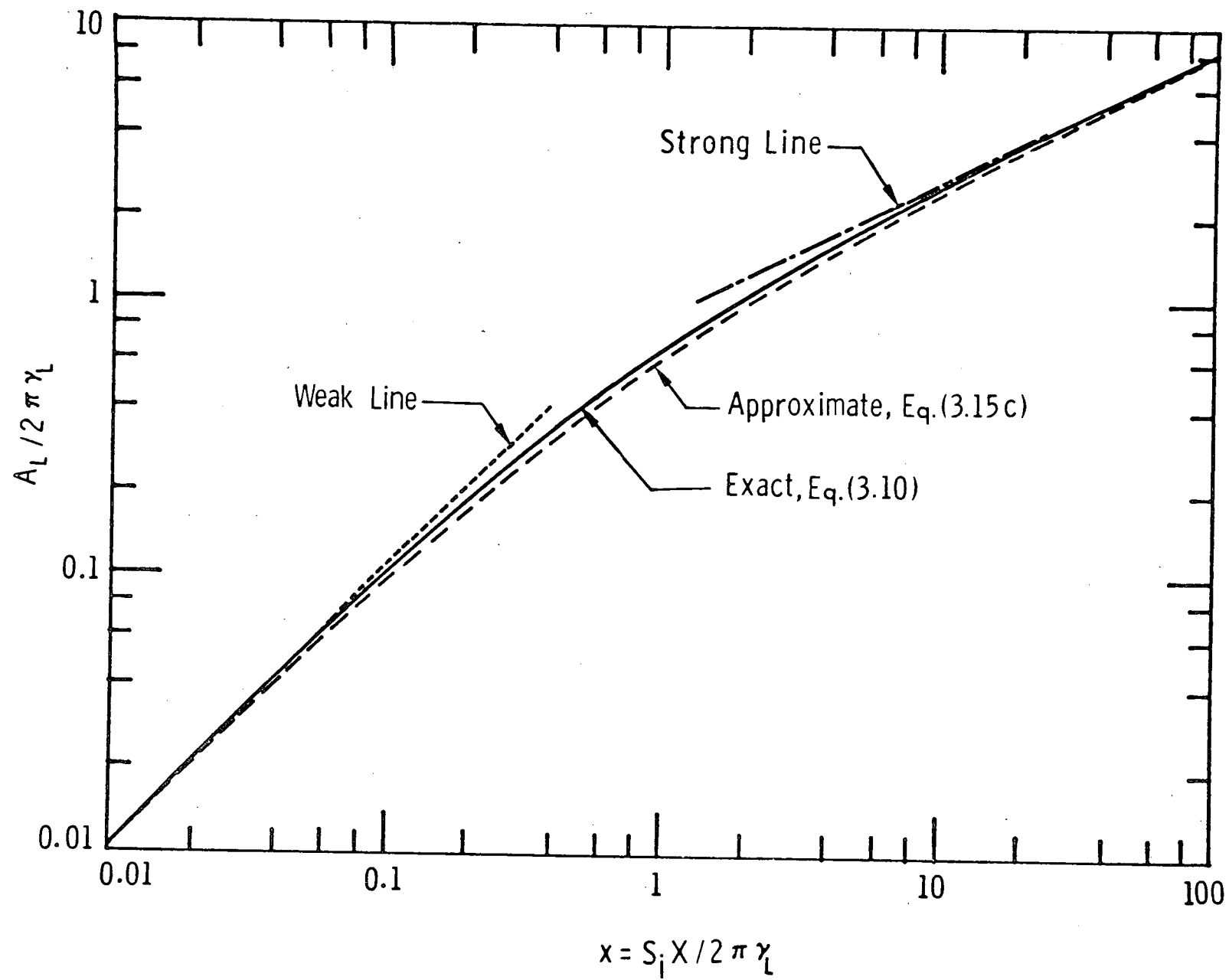$$A_D = (\pi/\ln 2)^{1/2} \gamma_D f(x_D) \, , \qquad (3.18a)$$

Fig. 2. Absorption by a single line of Lorentz shape

where

$$f(x_D) = \sum_{n=0}^{\infty} (-1)^n x_D^{n+1}/[(n+1)! \ (n+1)^{1/2}] \ . \qquad (3.18b)$$

This may be expressed in the nondimensional form

$$\bar{A}_D = A_D/[2\gamma_D/(\ell n2)^{1/2}] = (\sqrt{\pi}/2) \ f(x_D) \ . \qquad (3.19)$$

For $0.1 \leq x_D \leq 30$, Eq. (3.19) may quite accurately be approximated by

$$\bar{A}_D \simeq (\sqrt{\pi}/2) \ x_D \ \exp[-0.5 \ (x_D)^{1/2}] \ . \qquad (3.20)$$

As $x_D \to o$ (linear limit), Eq. (3.19) reduces to

$$\bar{A}_D = (\sqrt{\pi}/2) \ x_D \ , \qquad (3.21a)$$

or

$$A_D = S_j \ X \ . \qquad (3.21b)$$

This is identical to the result for the Lorentz profile in the linear limit (Eq. 3.11). Moreover, absorption by any line shape must reduce to this expression in the linear limit. This is because the linear limit can be obtained, independent of the line shape, directly from Eq. (3.6).

For large values of x_D, Eq. (3.19) may be expressed by an asymptotic expansion of the form

$$\bar{A}_D = (\ell n \ x_D)^{1/2} \{1-[1/2\Gamma(1/2)] \sum_{n=1}^{\infty} \Gamma^{(n)}(1) \ \Gamma \ (n-\tfrac{1}{2})/[n!(\ell n \ x_D)^n]\} \ , \qquad (3.22)$$

where $\Gamma^{(n)}(1)$ is the nth derivative of the gamma function evaluated at unit argument. In the limit of large x_D, this is further approximated by

$$\bar{A}_D \simeq (\ell n \ x_D)^{1/2} \ . \qquad (3.23)$$

It is important to note that in the limit of large x_D , the absorption increases very slowly with the amount of absorbing gas. This is because in the large path length limit the central portion of the line becomes opaque and absorption occurs solely in the line wings. Since the Doppler line shape drops off exponentially in the line wings, it is not possible to absorb much additional radiation in the wings by increasing the number of molecules.

The solutions expressed by Eqs. (3.19) and (3.20), as well as the limiting solutions, are illustrated in Fig. 3.
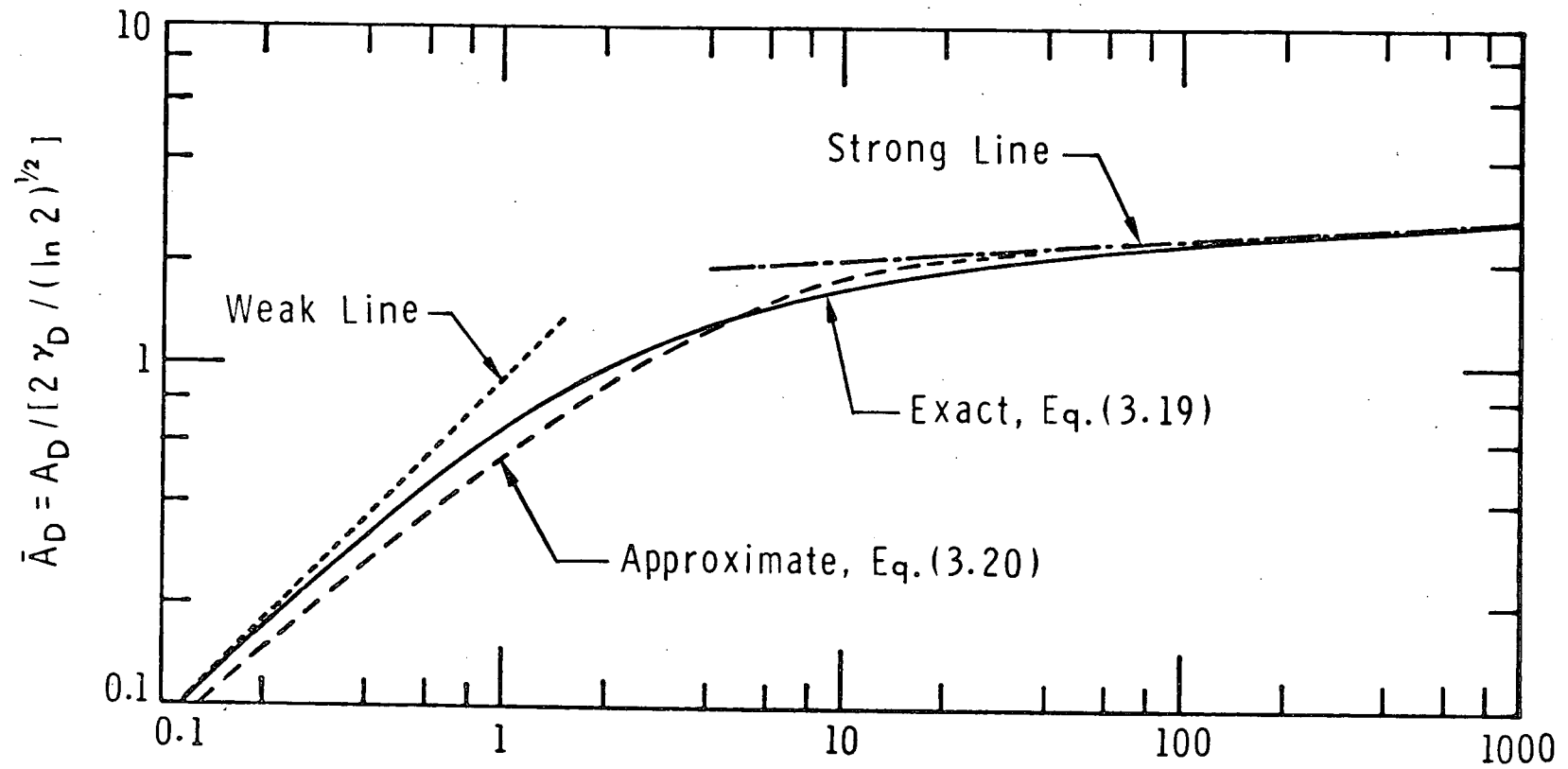
3. Lines with Combined Doppler and Lorentz Profile

For conditions where both the Doppler and the Lorentz broadenings are important, the total absorption, A_V , is obtained by combining Eqs. (2.12) and (3.6) as

$$\bar{A}_V = A_V / [2\gamma_D/(\ln 2)^{1/2}] = \frac{1}{2} \int_{-\infty}^{\infty} \{1 - \exp[-x_D K(a,v)]\}dv \quad . \tag{3.24}$$

It can easily be shown that Eq. (3.24) reduces to the Lorentzian case for large values of a and to the Doppler case in the limit of small a.

Numerical solution of Eq. (3.24) may be obtained by employing the appropriate expression for the Voight function, $K(a,v)$. Using the numerical procedure described by Young [18,19], Eq. (3.24) was solved for a range of the parameter a, and the results are illustrated in Fig. 4. Similar results were also obtained by Jansson and Korb [32], who employed a somewhat modified version of Armstrong's [17] Fortran IV program. These results are in general agreement with the results of Penner and Kavanagh [16]. As would be expected, for $a = o$, the results correspond to the case of a pure Dopper profile, while for $a > 10$ they correspond to the

The y-axis is labeled $\bar{A}_D = A_D / [2\,\gamma_D / (\ln 2)^{1/2}]$

Labels within the figure: Strong Line, Weak Line, Exact, Eq. (3.19), Approximate, Eq. (3.20)

The x-axis equation:

$$X_D = \kappa_o X = [(S_i / \gamma_D)(\ln 2 / \pi)^{1/2}]\, X$$

Fig. 3. Absorption of a single line of Doppler profile

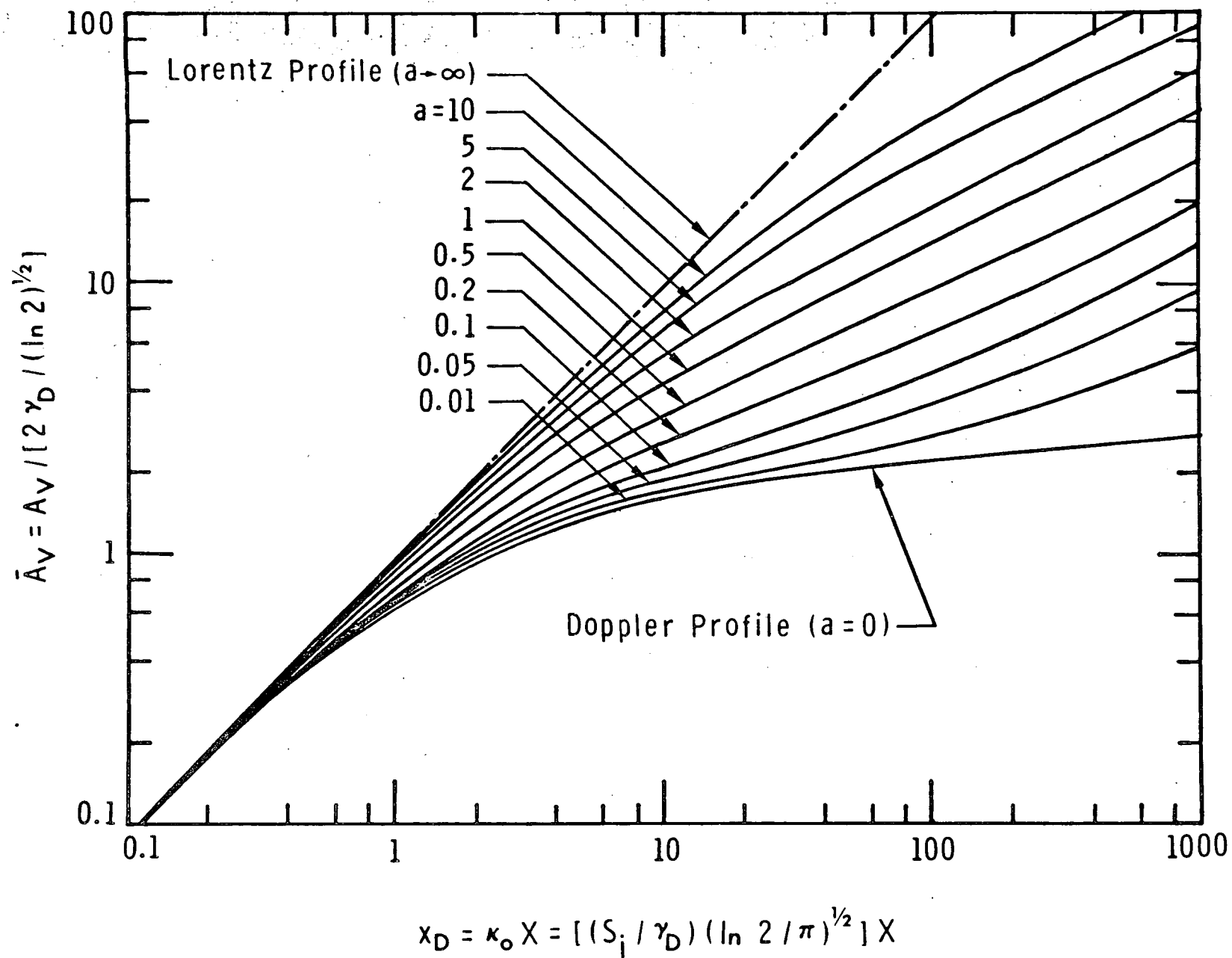Fig. 4. Absorption of a single line of Voight shape

The figure shows a log-log plot. The vertical axis is labeled $\bar{A}_V = A_V / [2\gamma_D / (\ln 2)^{1/2}]$ ranging from 0.1 to 100. The horizontal axis ranges from 0.1 to 1000 and is labeled below:

$$x_D = \kappa_o X = [(S_i / \gamma_D)(\ln 2 / \pi)^{1/2}] X$$

Curves are labeled:

Lorentz Profile $(a \rightarrow \infty)$
$a = 10$
5
2
1
0.5
0.2
0.1
0.05
0.01

Doppler Profile $(a = 0)$

Lorentzian shape.

If the approximate relation for a Voight Profile, as given by Eq. (2.21), is employed, then the total line absorption, A_W , is expressed by

$$\bar{A}_W = A_W / [2\gamma_D / (\ell n2)^{1/2}] = \frac{1}{2} \int_{-\infty}^{\infty} \{1 - \exp[-x_D W(a,v)]\}dv , \qquad (3.25)$$

where

$$W(a,v)/[(\ell n2/\sqrt{\pi})F(a)] = [1-(\gamma_L/\gamma_V)] \exp\{-11.088[(v/a)(\gamma_L/\gamma_V)]^2\}$$

$$+ (\gamma_L/\gamma_V)/\{1 + 16[(v/a)(\gamma_L/\gamma_V)]^2\} ,$$

$$F(a) = \{a[1.065/(\gamma_L/\gamma_V) + 0.447 + 0.058 (\gamma_L/\gamma_V)]\}^{-1} ,$$

$$(\gamma_L/\gamma_V) = \{0.5 + [0.25 + (\ell n2/a^2)]^{1/2}\}^{-1} .$$

The numerical solution of Eq. (3.25) is straightforward. In Fig. 5, some results of Eq. (3.25) are compared with the solutions obtained by using the actual Voight profile. Except for very small values of the parameter a , the agreement between the two solutions is quite satisfactory.

4. Comparison of Integrated Line Absorption

The errors, in the integrated line absorption, encountered in using the Lorentz shape to approximate the Voight profile, are illustrated in Fig. 6 for a range of the parameter a . As would be expected, maximum errors occur for intermediate path lengths and for lower values of a . The errors, however, are not significant in the two limiting cases of small and large path lengths. As discussed earlier, for small path lengths (linear limit), the line absorption is independent of the line shapes. In the limit of large path lengths, however, the central
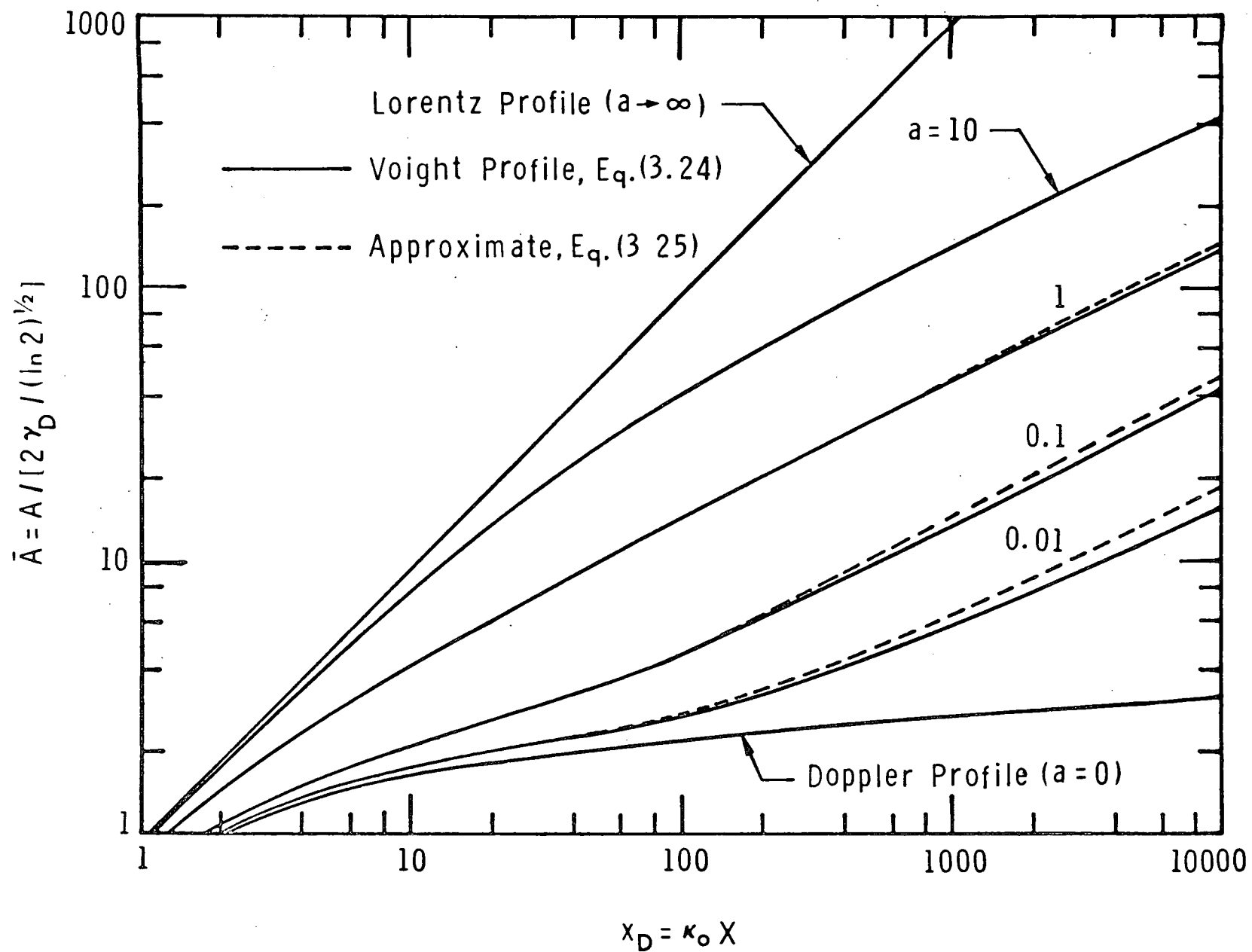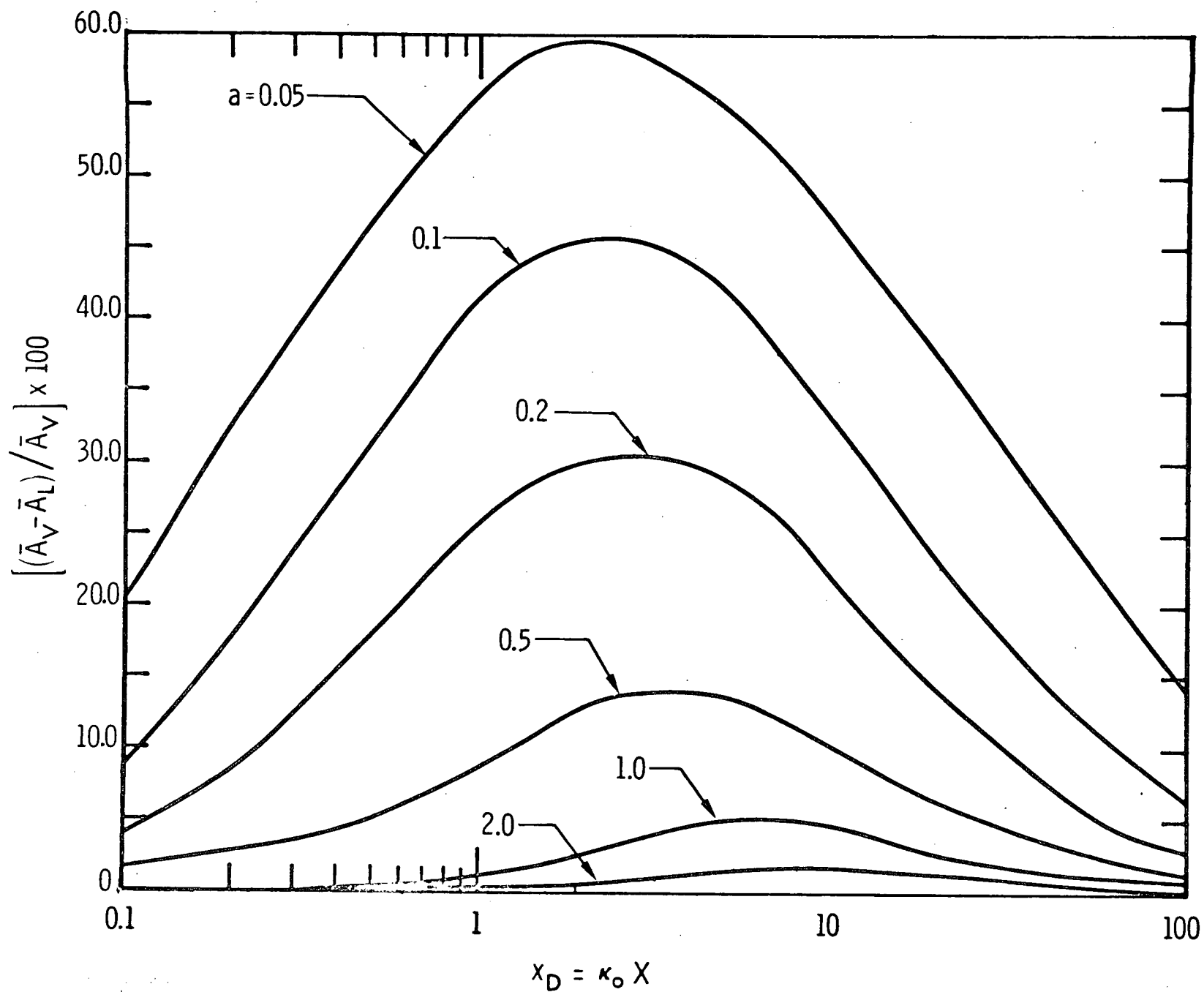
Fig. 5. Comparison of line absorptance

Fig. 6. Errors in the absorption by using the Lorentz line shape
instead of the Voight line profile

portion of the line becomes opaque and absorption occurs only in the wing regions. Since the Voight profile is essentially Lorentzian in the line wings, the error encountered in the large path length limit becomes insignificant.

The errors resulting from using the Doppler line profile to approximate the absorption by the Voight line profile are illustrated in Fig. 7. Since $a = o$ corresponds to the case of pure Doppler absorption, the errors are expected to be higher for larger values of a . Maximum errors, in this case, are found in the large path length limit. This is because, in this limit, the absorption occurs essentially in the line wings and the Voight profile in the wing regions is Lorentzian rather than of Doppler shape.

It should be emphasized that for cases of intermediate path lengths and for moderate values of a $(0.1 < a < 10)$ the use of the Voight profile becomes almost essential. This situation corresponds to the radiative transmittance in the earth's troposphere and lower stratosphere. Consequently, for radiative modeling of the lower atmosphere, consideration must be given to the application of combined line profiles.

In Figs. 8 - 12, comparisons of results for all three line profiles (Lorentz, Doppler, and Voight) are made for $a = 0.001$, 0.01, 1.0, and 10. These figures clearly illustrate the range of validity of the absorption by the three line profiles. In Figs. 8 - 10, the curves for $\bar{A}_L$ and $\bar{A}_D$ intersect at some point, say x_{DI}, the location of which increases with decreasing a . For $a > 2$, $\bar{A}_L$ and $\bar{A}_D$ curves do not intersect, and $\bar{A}_L$ and $\bar{A}_V$ curves become identical for almost all path lengths.
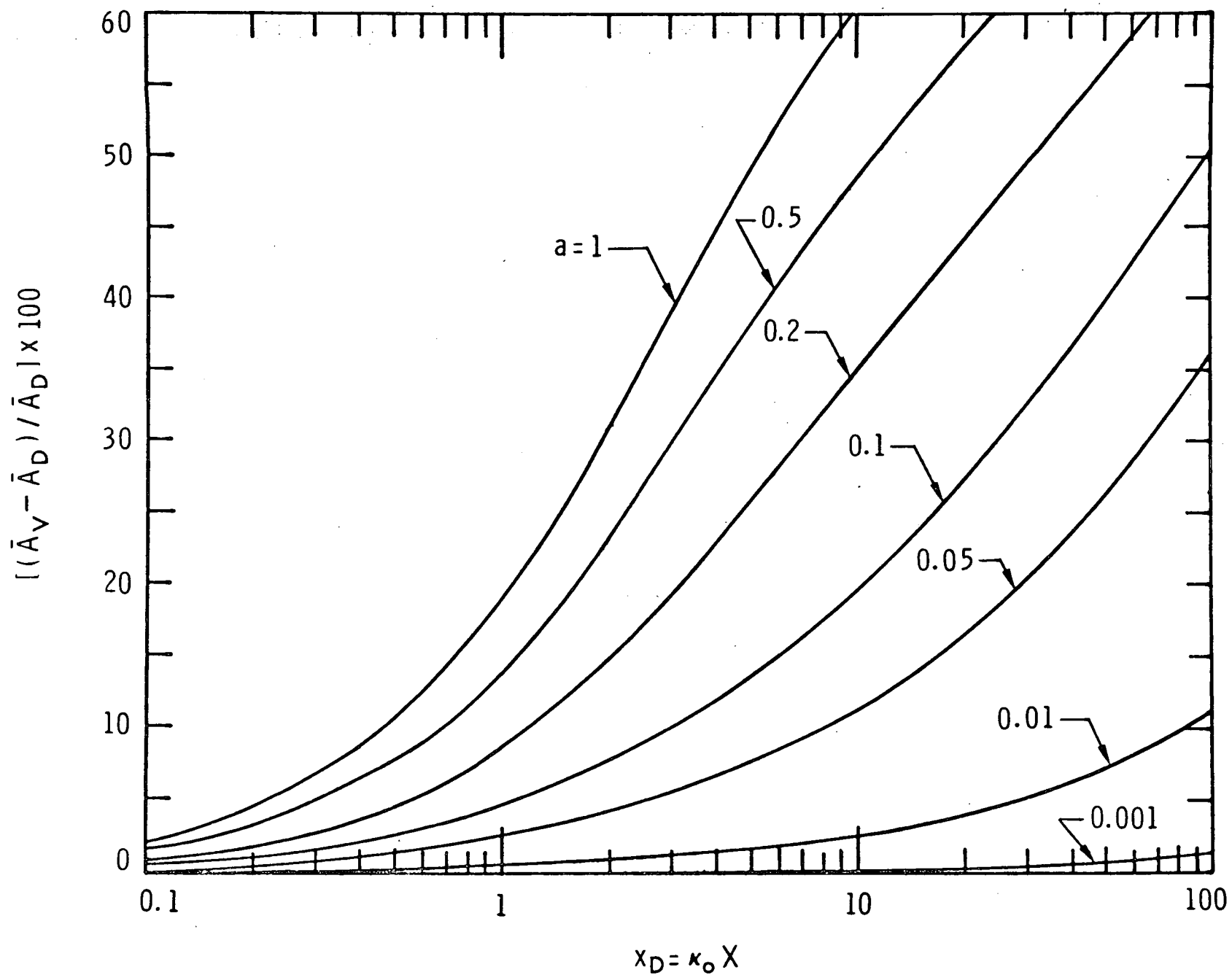
Fig. 7. Errors in the absorption by using the Doppler line shape instead of the Voight line profile

Yamada [33] has reported that $\bar{A}_L$ and $\bar{A}_V$ curves became identical for $a > 0.2$ which is not in agreement with the present investigation. It should be realized, however, that the parameter a is a measure of the relative importance of Lorentz versus Doppler effect. For a value of $a = 0.5$, for example, the ratio of Lorentz to Doppler width, $(\gamma_L/\gamma_D) = a/\sqrt{\ln 2} \simeq 0.6$. In this case, therefore, the Doppler effect will be significant especially for the intermediate path lengths and integrated absorption could not be expressed solely in terms of the absorption by Lorentzian profile. It is quite possible that the way Yamada's results were illustrated, the difference between $\bar{A}_L$ and $\bar{A}_V$ curves was not apparent in the intermediate path lengths. For small as well as large path lengths, $\bar{A}_L$ and $\bar{A}_V$ are, of course, identical.
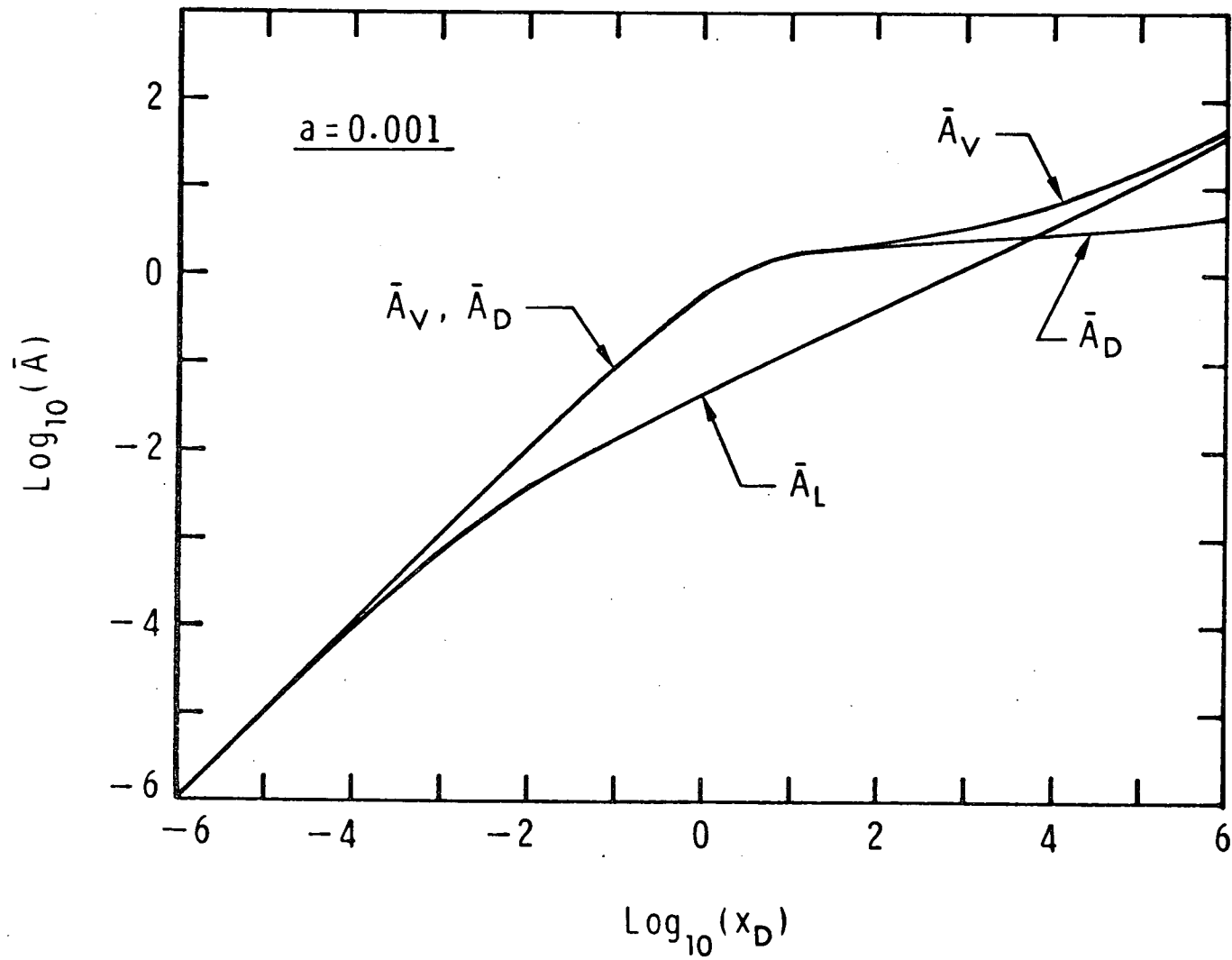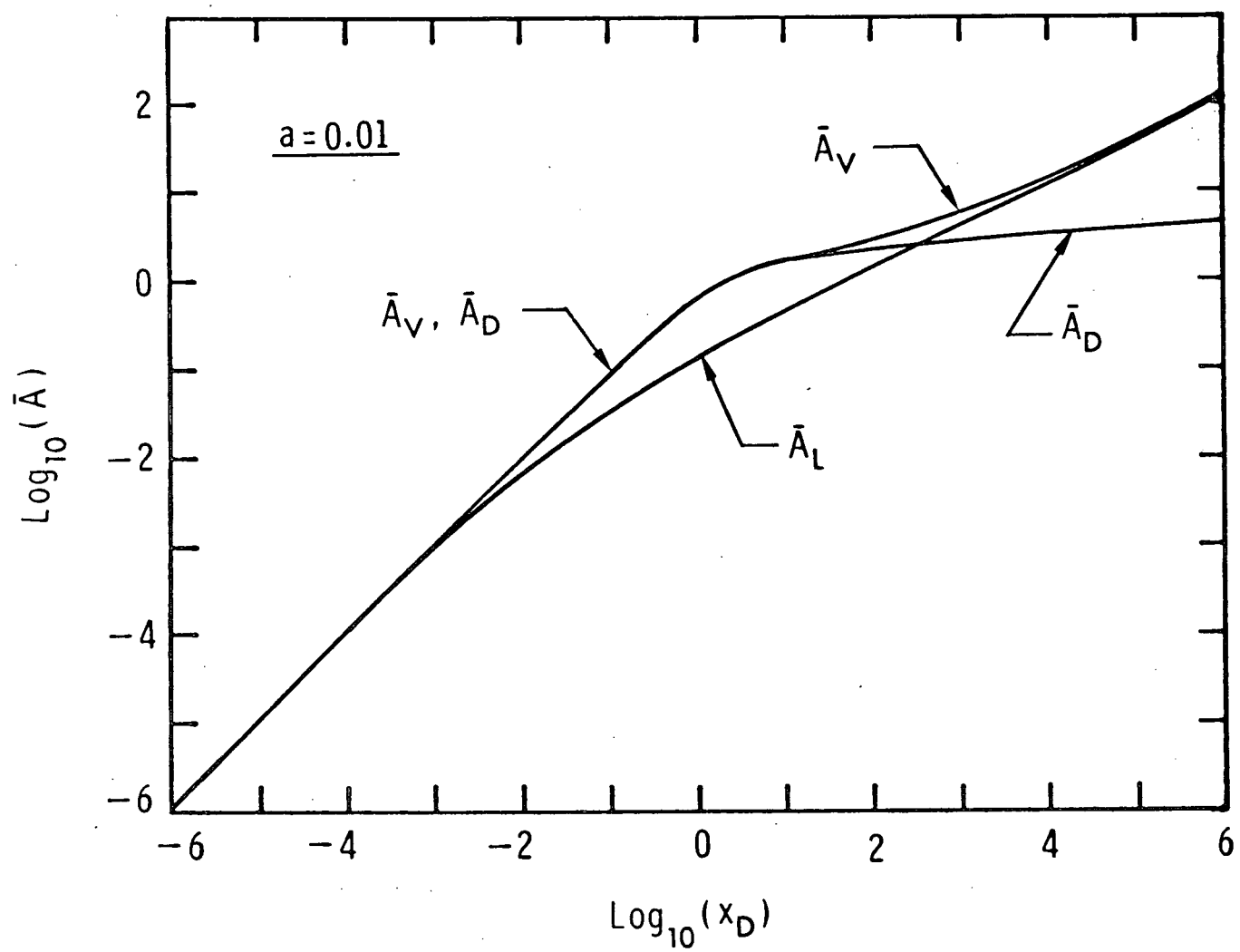
Fig. 8. Comparison of line absorption for a = 0.001
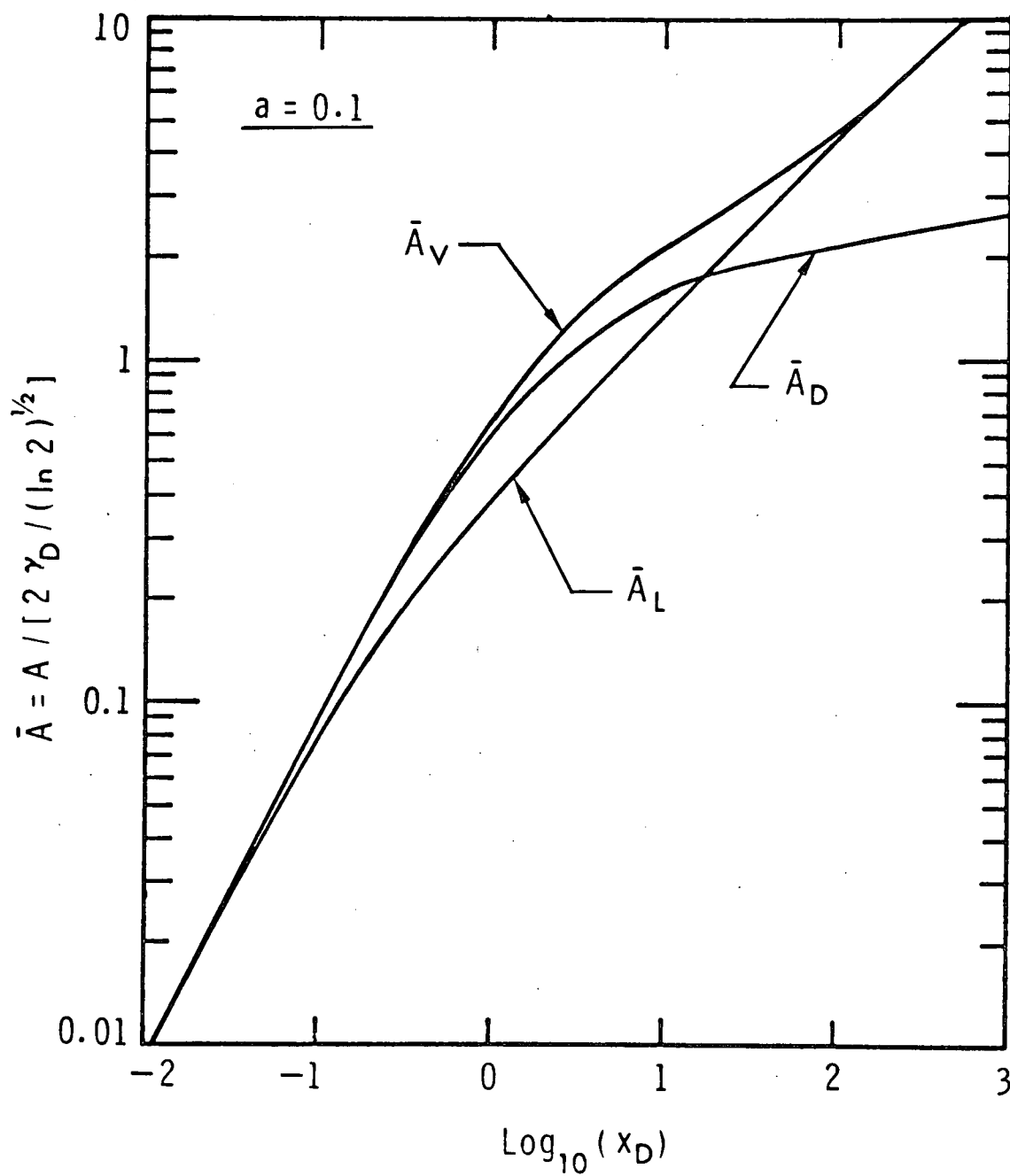
Fig. 9.   Comparison of line absorption for a = 0.01
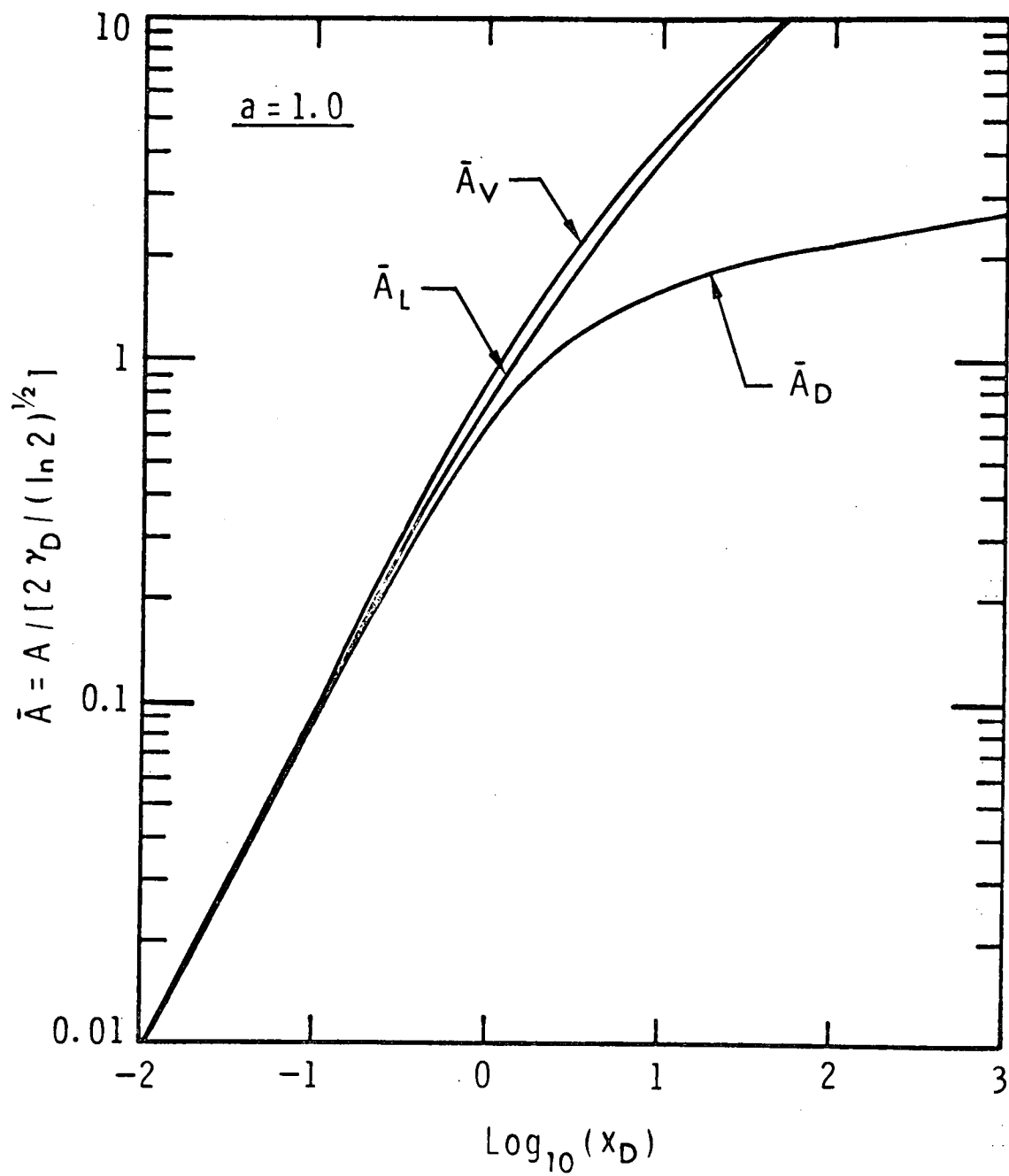
Fig. 10. Comparison of line absorption for a = 0.1
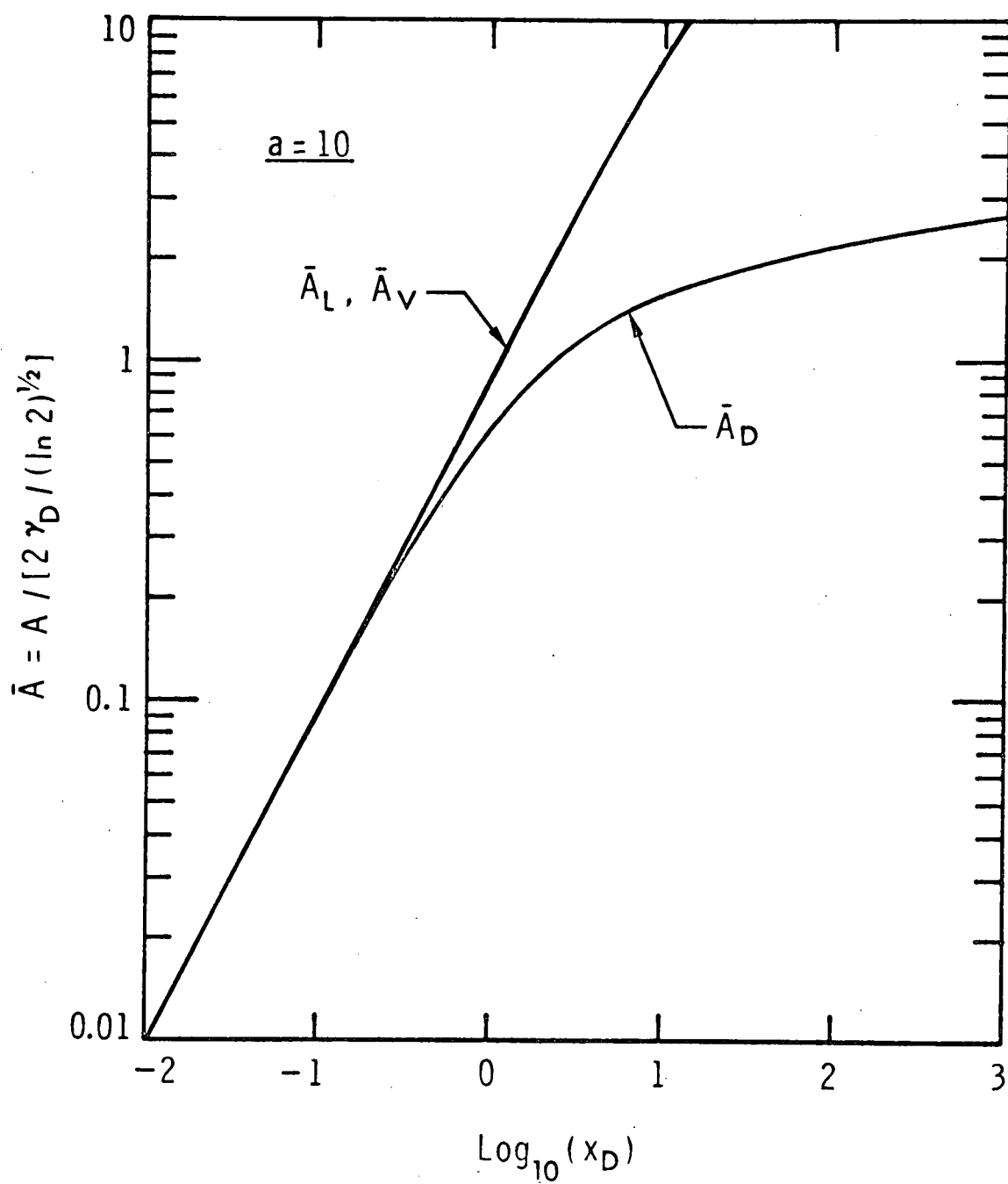
Fig. 11. Comparison of line absorption for a = 1.0

Fig. 12. Comparison of line absorption for a = 10.

IV. REVIEW OF BAND MODELS AND BAND ABSORPTANCE CORRELATIONS

The absorptions by atmospheric gases, under certain atmospheric conditions, result in overlapping spectral lines. Thus, the total absorption within certain frequency interval cannot accurately be represented simply by summing the absorption by individual lines. This is because the absorption in a region of overlapped lines is always less than the absorption calculated by considering the contributions of individual non-overlapping lines.

The total absorption of a band of overlapping lines strongly depends upon the line intensity, the line half-width, and the spacing between the lines. In a particular band, the absorption coefficient varies very rapidly with the frequency and, therefore, it becomes a very difficult and time-consuming task to evaluate the total band absorptance by numerical integration over the actual band contour. Consequently, several approximate band models have been proposed which represent absorption from an actual band with reasonable accuracy.

1. Elsasser Band Model

The simplest band model that accounts for the line structure is the Elsasser model [26], for which equally spaced lines of equal intensity and equal half width are assumed. The expression for the total band absorption by Elsasser band model has been developed only for lines having the Lorentz line profile. For homogeneous atmosphere, the total absorptance of the Elsasser band is found to be [5,27]

$$A = (A_o/2) \int_0^2 \{1 - \exp[- \frac{u \sinh(\pi\beta/2)}{\cosh(\pi\beta/2) - \cos(\pi z/2)}]\} \, dz , \qquad (4.1)$$

where

$$A_o = nd \ , \quad u = Spy/A_o \ , \quad \beta = 4\gamma_L/d \ , \quad z = 4(\omega-\omega_o)/d \ .$$

In this equation u is the dimensionless pressure path length, β is the line structure parameter, A_o is the band width parameter, n is the number of lines in the band, and d is the spacing between the lines. Equation (4.1) has a form that is characteristic of all band models, namely that the total absorptance may be expressed as

$$A = A_o \bar{A}(u,\beta) \ , \tag{4.2}$$

where $\bar{A}(u,\beta)$ is a dimensionless function. Equation (4.1) reduces to several limiting forms which are discussed in [5]. By employing the scaling approximations mentioned in references [34-37], Eq. (4.1) may be used to evaluate the total band absorptance for the case of hon-homogeneous atmosphere.

2. Statistical (Mayer - Goody) Band Model

The statistical band model is based upon the assumption that, in a given wave number interval, the spectral lines are randomly spaced and that the intensity of these lines can be specified by some distribution function. For this model, the absorptance over a wave number interval, $D = nd$, is given by [27-29]

$$A = 1 - (1 - \bar{A}_{j,D})^n \tag{4.3}$$

where n is the number of lines in interval D, d is the mean spacing between the lines, and

$$\bar{A}_{j,D}(S_o,X,p) = \int_o^\infty A_{j,D}(S,X,p) \ P(S,S_o)dS. \tag{4.4}$$

In Eq. (4.4), A_j,D is the absorptance of a single line over the entire

wave number interval D , $P(S,S_o)$ is the normalized probability of

finding a spectral line with an intensity between S and $S + dS$, and

S_o is the parametric line intensity that occurs in the intensity dis-

tribution function.

By employing one definition of the exponential, it may be shown

that for large number of lines in the interval D, Eq. (4.3) becomes [29]

$$A = 1 - \exp(-n \, \bar{A}_{j,D}) \, , \qquad n \gg 10 \qquad (4.5)$$

If it is assumed that all lines, within the wave number interval

D , are equally intense then

$$P(S) = \delta(S - S_o) \qquad (4.6)$$

and it follows that

$$\bar{A}_{j,D}(S_o,X,p) = A_{j,D}(S_o,X,p) \qquad (4.7)$$

Now, the expression for $A_{j,D}$ can be obtained from Section-III for

a particular line shape simply by replacing S by S_o.

The development of the expressions for absorption by a single

isolated line, in Section-III, assumes an infinite wave number interval.

Consequently, these expressions can be used in Eqs. (4.4) and (4.5) only

if there is no appreciable absorption by the individual line beyond wave

number interval D. If this is not the case then the expression for

$A_{j,D}$ should be obtained by integrating the expression for the line

absorption over the actual frequency interval D.

If an exponential distribution of line intensities is assumed, then

$$P(S) = \exp(-S/S_o)/S_o \qquad (4.8)$$

and, for a particular line shape, the line absorption can be calculated by using this line intensity distribution. For spectral lines with Lorentz shape, the absorption by the statistical band model, in this case, is found to be [29]

$$A = 1-\{1-(\pi\beta x_o/2)/n(1 + 2x_o)^{1/2}\}^n \qquad (4.9)$$

or

$$A = 1-\exp\{-(\pi\beta x_o/2)/(1 + 2x_o)^{1/2}\} \text{ for } n \gg 10 , \qquad (4.10)$$

where

$$x_o = S_o X/2\pi\gamma_L$$

Since the lines are assumed to be randomly distributed in the statistical model, the absorption by this model is always less than that by the Elsasser band model. The advantage of the statistical model is that it can be applied to any line shape.

3. Random Elsasser Band Model

In actual vibration-rotation bands, lines are arranged neither completely at random nor at regular intervals. Within a band, there may be a number of strong lines in certain narrow spectral region while in other regions only very weak lines may be present. There may also occur a superposition of equally intense lines in another spectral region of the band. In cases like this, a more accurate representation of band absorption is provided by the random Elsasser model, which assumes the random superposition of several different Elsasser bands. Each of the superposed bands may have different line intensities, half-widths, and spacing. As many different Elsasser bands as necessary may be superimposed in this model. As the number of superposed Elsasser bands becomes large,

the absorption by the entire band approaches that given by the statistical

band model. For N randomly superposed Elsasser bands, the absorption

is given by the relation [27,29,38]

$$A = 1 - \prod_{i=1}^{N} [1 - A_{E,i}(x_i, \beta_i)] \tag{4.11}$$

where $A_{E,i}$ is the absorptance of an Elsasser band.

4. Quasi-Random Band Model

Quasirandom model is probably the best model to represent the
absorption of a vibration-rotation band quite accurately. It assumes
neither a regular nor a random spacing of the spectral lines. The
essential feature of this model is to divide the wider frequency
interval of the actual band into much narrower subintervals. In each
of these subintervals, the spectral lines are assumed to have random
spacing. In this manner, the model accounts for the actual intensity
distribution of strong as well as weak spectral lines. The absorption
of the narrow spectral interval is calculated from the relation of a
single-line absorption over a finite interval. The absorption of each
of the n lines in the narrow interval is calculated separately and
the results are combined by assuming a random position for the lines
within the interval. The total band absorptance is calculated by averaging
the results from the smaller intervals.

The total band absorptance of a quasirandom band model is given
by the expression [39]

$$A = \frac{1}{\delta} \sum_{K=1}^{\delta} A_K \tag{4.12}$$

where

$$A_\kappa = 1 - \prod_{i=1}^{M} [1 - A_{j,D}^{(i)}(S_i,d_i)] \qquad (4.13)$$

In these equations, δ is the width of the narrow frequency intervals and A_κ is the corresponding absorptance of each subinterval. $A_{j,D}^{(i)}$ is the absorptance of a single line over the finite interval D and M is the number of lines in the frequency interval κ.

The four band models reviewed above are called the narrow band models. There are three limits in which approximate expressions for the total band absorptance, by these bands, can be obtained. These are weak-line approximation, strong-line approximation, and nonoverlapping-line approximation. These approximations are discussed in detail in reference [40].

The narrow band models may be employed to compute the transmittance from atmospheric gases under most atmospheric conditions. Before the use of these band models can be justified, however, it would be advisable to compare them with the line-by-line model especially for gases whose line parameters are completely known.

5. Wide Band Models

Aside from the narrow band models discussed above, there are also available in literature the so-called wide band models which provide correlations that are valid over the entire band pass. Besides possessing the conventional linear and square-root limits, these models also possess another asymptotic limit which is called the logarithmic limit. Even though the use of these models may be restricted for atmospheric applications, they do provide a quick and accurate information regarding

transmittance of gases at moderately high temperatures. As such, these models are quite useful in many engineering applications.

a) <u>The Box Model</u>: The simplest of the wide band models is the box model which was first introduced by Penner [10]. For this model, it is assumed that the absorption coefficient, κ_ω , is constant over an effective band width $\Delta\omega$. The expression for the total absorptance by this model is given as

$$A = \int_{\Delta\omega} [1 - \exp(-\kappa_\omega X)] \, d\omega = (\Delta\omega)_e [1 - \exp(-\bar{\kappa}X)]$$

where $(\Delta\omega)_e$ is the effective band width, and $\bar{\kappa}$ is the mean absorption coefficient for the interval $(\Delta\omega)_e$. Further discussion and application of the box model is available in references [10,31,41] .

b) <u>The Exponential Wide Band Model</u>: Edwards and his co-workers [4,42] have considered various wide band models (Rigid rotator, non-rigid rotator, and Arbitrary models) and have concluded that three parameters (the mean line intensity to spacing ratio, the mean line-width to spacing ratio, and the effective broadening pressure) are necessary for a complete description of the band absorption. For complete discussions of these models and their limiting forms, one should refer to [4,5,31,42]. By using the Curtis-Godson approximation, the exponential wide band model can be applied to calculate the band absorption for nonhomogeneous gases.

6. <u>Band Absorptance Correlations</u>

Three continuous relations, for the total band absorptance, which are valid over all values of path lengths and line structure para-meters, are available in literature [5,31,43]. These are,

(a) Tien and Lowder:

$$\bar{A} = A/A_o = \ln(uf(\beta)\{(u + 2)/[u + 2f(\beta)]\} + 1) \ ,$$

where

$$f(\beta) = 2.94[1 - \exp(-2.60\beta)] \ ,$$

(b) Goody and Belton:

$$\bar{A} = 2 \ln\{1 + [u\sqrt{\beta}/(u + 4\beta)^{1/2}]\} \ ,$$

(c) Cess and Tiwari:

$$\bar{A} = 2 \ln\{1 + u/[2 + \sqrt{u(1 + 1/\beta)}]\} \ .$$

Various limitations as well as applications of these correlations are discussed in [5].

By employing either an appropriate line or band model, the total (integrated) band absorptance can be obtained for a range of atmospheric parameters. It would be interesting to compare the band absorptance results obtained by using different line and band models.

V. EXPRESSIONS FOR UPWELLING ATMOSPHERIC RADIATION

As shown in Fig. 13, the radiation emergent from the atmosphere, $E(\omega)$, may be given by the expression [44]

$$E(\omega) = E_G(\omega) + E_R(\omega) + E_\phi(\omega) + E_{R\phi}(\omega) \qquad (5.1)$$

where

$E_G(\omega)$ = thermal radiation emitted by underlying surface and

atmosphere

$E_R(\omega)$ = incident solar radiation reflected by the surface

$E_\phi(\omega)$ = radiation scattered by a single or multiple scattering

processes in the atmosphere without having been

reflected from the surface

$E_{R\phi}(\omega)$ = scattered energy which has undergone a reflection from

the surface.

In general, these quantities are functions of surface temperature, atmospheric temperature, surface emittance, surface reflectance, sun zenith angle, scattering characteristics of particles, and transmittance of the atmosphere.

Neglecting the scattering and solar radiation, the equation of radiative transfer for thermal radiation emerging from a plane-parallel atmosphere, with underlying surface of emittance $\varepsilon(\omega)$, can be written as

$$E(\omega) = E_G(\omega) = \varepsilon(\omega) \, B(\omega,T_s) \, \tau(\omega,o)$$
$$+ \int_o^h B(\omega,T(z)) \, [d\tau(\omega,z)/dz]dz \qquad (5.2)$$

where $B(\omega,T)$ is the Planck's blackbody function, T_s is the surface temperature, $T(z)$ is the temperature at altitude z, and $\tau(\omega,z)$ is the
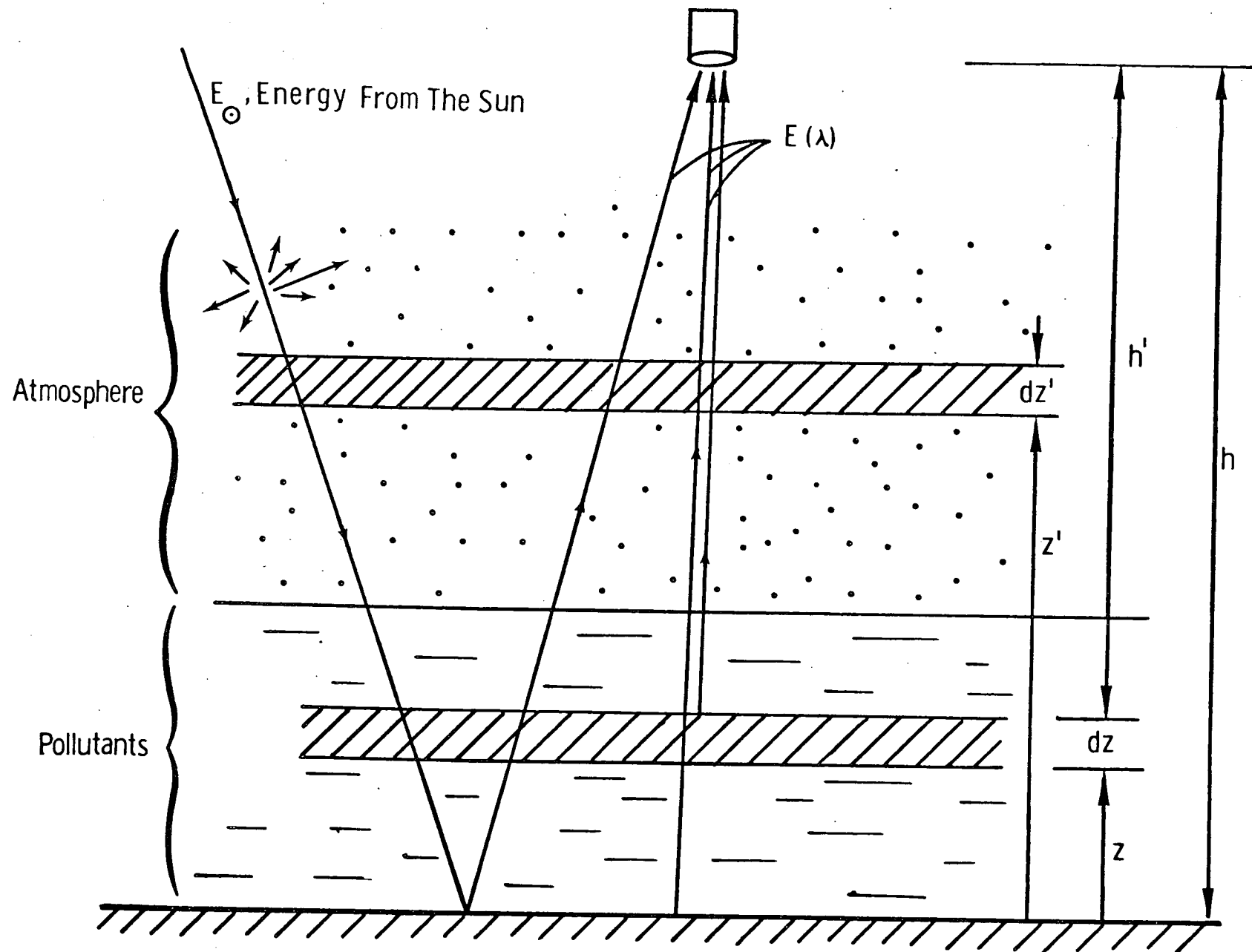
Fig. 13. Energy received by an aircraft or satellite mounted instrument

monochromatic transmittance of the atmosphere (at wave number ω)
between altitude z and the top of atmosphere.

The contribution from sunlight reflected from the surface
becomes significant at shorter wavelengths. This contribution is
given by the component $E_R(\omega)$ as

$$E_R(\omega) = (1/\pi)[1 - \varepsilon(\omega)] \cos \theta \; H_s(\omega) [\tau(\omega)]^\zeta \qquad (5.3)$$

where θ is the sun zenith angle and $\zeta = 1 + f(\theta)$. Function
$f(\theta) = \sec \theta$ for $o \leq \theta \leq 60°$ and equals to $Ch \; \theta$ for $\theta > 60°$ with
$Ch \; \theta$ denoting the Chapman function. $H_s(\omega)$ is the sun irradiance on
top of the atmosphere, and $\tau(\omega)$ is the transmission vertically through
the atmosphere.

The expression for the transmittance $\tau(\omega,z)$ is obtained from
an appropriate molecular (band or line) model considered in the previous
sections. In general, the transmittance may be expressed as

$$\tau(\omega,z) = \prod_i [\tau_i(\omega,z)] = \exp[- \int_o^z \sum_i \beta_i(\omega,z') \; n_i(z') \; dz'] \qquad (5.4)$$

where $\beta_i(\omega,z)$ is the extinction coefficient for species i which is
equal to the sum of absorption and scattering coefficients, and n_i is
the number density of the contributing molecules of species i in the
optical path.

A combination of Eqs. (5.1) through (5.4) yields a relation for
thermal radiation emerging from a plane-parallel atmosphere. This
equation, with appropriate spectroscopic information, can be used to
reduce the measured atmospheric data by an inversion procedure. The
equation may also be used to obtain the concentration of atmospheric

pollutants, from radiation measurements, provided other governing parameters are known.

In radiation modeling for pollution measurement, the upwelling radiation from the nonhomogenous atmosphere is calculated by dividing the atmosphere into an appropriate number of sublayers. Each of these sublayers is assumed to be homogeneous in species concentration, temperature and pressure.

It should be noted that the derivation of Eq. (5.2) assumes the existence of local thermodynamic equilibrium. This assumption, however, is not justified for gases like carbon monoxide for the range of atmospheric pressures and temperatures. Since the nonequilibrium effect comes only through the source function [27,45], for gases like CO, the Planck function in Eq. (5.2) should be replaced by the nonequilibrium source function. The use of Eq. (5.2) is, however, justified for gases like CO_2, Ch_4, and H_2O.

VI. CONCLUDING REMARKS

The purpose of this study was to compare the total (integrated) absorptions of the three line profiles, Lorentz, Doppler, and Voight, for a range of the governing parameters. It is concluded that the Voight line profile should be employed in calculating the transmittance for the troposphere and lower stratosphere. Line-by-line models are preferred over band models for atmospheric applications. The line-by-line model is especially convenient in cases where there is interference of other species within the spectral region of interest.

The equation for the radiative transmittance, based on the line-by-line model, is used in the expressions for upwelling radiation which is received by an aircraft or satellite mounted instrument. From these radiation measurements, amounts of atmospheric pollutants are determined by employing an appropriate data reduction scheme. The essential parameters, appearing in actual calculation of the amount of each pollutant, are: ground temperature, ground emissivity, sun zenith angle, atmospheric temperature profile, water vapor distribution, and distribution of interfering species. Furthermore, within the spectral region of each pollutant, there may appear several thousand spectral lines. Thus, time required for data reduction becomes quite large. One way to reduce the data reduction time will be to employ an appropriate narrow band model in place of the line-by-line model. If the spectral region of interest could be divided into a number of convenient narrow spectral intervals, then it is quite possible that either the statistical or quasi-random band model would provide an accurate description of the entire spectral transmittance. However, before these band models can be employed for atmosphere applications, their

validity must be established by comparing the transmittance of these models

with the results obtained by using the line-by-line model.

LIST OF SYMBOLS

a	parameter representing the ratio of Lorentz to Doppler width, Eq. (2.10)
A	total band absorptance, cm^{-1}
$\bar{A}$	dimensionless band absorptance
A_D	total absorptance of a single Doppler line
$\bar{A}_D$	dimensionless A_D
$A_{E,i}$	absorption of a narrow Elsasser band
A_j	total absorption of a single line (jth line)
$A_{j,D}$	absorption of a single line over wave number interval D
A_L	total absorption of a single Lorentz line
$\bar{A}_L$	dimensionless A_L
A_o	band width parameter, cm^{-1}
A_V	total absorption of a single Voight line
$\bar{A}_V$	dimensionless A_V
A_W	total absorption of a single line given by Eq. (3.25)
$\bar{A}_W$	dimensionless A_W
$B(\omega,T)$	Planck's function
c	speed of light
E	upwelling radiative energy
E_G	thermal radiation of ground and atmosphere
E_R	solar radiation reflected from ground
E_ϕ	solar radiation scattered by the atmosphere without having been reflected by the ground
$E_{R\phi}$	solar radiation reflected from ground outside the field of view and scattered by the atmosphere into the field of view

h	altitude of an aircraft or a satellite
H_s	sun irradiance at the top of the atmosphere
κ	Boltzmann constant
$K(a,v)$	Voight function, Eq. (2.12)
m	molecular mass of the absorbing medium
p,P	partial pressure of the absorbing medium
S_j	line intensity or line strength, cm^{-2}
T	kinetic temperature, °K
T_s	surface or ground temperature
$T(z)$	temperature of the atmosphere at altitude z
u	dimensionless coordinate, $u = Spy/A_o$
v	wave number scaling factor, Eq. (2.11)
X	mass of absorbing gas per unit area
x	optical path at the line center, Eq. (3.8a)
x_D	optical path at the line center, Eq. (3.18a)
x_o	optical path at the line center, Eq. (4.10)
β	line structure parameter
γ	line half-width of a spectral line
γ_D	Doppler line half-width
γ_L	Lorentz line half-width
γ_V	Voight line half-width
ε	surface emittance
θ	sun zenith angle
κ_o	absorption coefficient correlation, Eq. (2.13), cm^{-1}
κ_ω	equilibrium spectral absorption coefficient, cm^{-1}
$\kappa_{\omega j}$	absorption coefficient of jth spectral line

$\kappa_{\omega o}$ spectral absorption coefficient correlation, Eq. (2.23).

τ radiative transmittance

τ_{ω} spectral transmittance

ω wave number, cm^{-1}

ω_{j} wave number at the line center

REFERENCES

1. W. S. Benedict, R. Herman, G. E. Moore, and S. Silverman, Ap. J. <u>135</u>, 277 (1962).

2. S. R. Drayson and C. Young, Tech. Report, Dept. of Aerospace Engineering, University of Michigan, Ann Arbor (1967).

3. W. S. Benedict and R. F. Calfee, ESSA Prof. Paper 2, Washington, D. C., (1967).

4. D. K. Edwards, L. K. Glassen, W. C. Hauser, and J. S. Tuchscher, J. Heat Transfer <u>86</u>, 219 (1967).

5. R. D. Cess and S. N. Tiwari, "Infrared Radiative Energy Transfer in Gases," Advances in Heat Transfer Vol. VIII, Academic Press, New York (1972).

6. S. R. Drayson, Applied Optics <u>5</u>, 385 (1966).

7. G. Yamamoto, M. Tanaka, and T. Aoki, J. Quant. Spectrosc. Radiat. Transfer <u>9</u>, 371 (1969).

8. R. Ely and T. K. McCubbin, Jr., Applied Optics <u>9</u>, 1230 (1970).

9. L. D. Tubbs and D. Williams, J. Opt. Soc. Amer. <u>62</u>, 284 (1972).

10. S. S. Penner, "Quantitative Molecular Spectroscopy and Gas Emissivities," Addison-Wesley, Reading, Massachusetts, 1959.

11. A. C. G. Mitchell and M. W. Zemansky, "Resonance Radiation and Excited Atoms, Cambridge Univ. Press., Cambridge, 1934.

12. F. Reiche, Verhandl. deut. Physik. Ges. <u>15</u>, 3 (1913).

13. G. N. Plass and D. I. Fivel, Astrophy. J. <u>117</u>, 225 (1953).

14. M. Born, Optik, pp 482-486, Julius Springer, Berlin (1933).

15. D. L. Harris III, _Astrophys. J._ 108, 112 (1948).

16. S. S. Penner and R. W. Kavanagh, _J. Opt. Soc. Amer._ 43, 385 (1953).

17. B. H. Armstrong, _J. Quant. Spectrosc. Radiat. Transfer_, 7, 61 (1967).

18. C. Young, _J. Quant. Spectrosc. Radiat. Transfer_, 5, 549 (1965).

19. C. Young, "Table for Calculating the Voight Profile," Univ. of
    Michigan, College of Engineering Report 05863-7-T, Ann Arbor,
    Mich. (1965).

20. D. H. Hummer, "The Voight Function: An Eight-Significant-Figure
    Table and Generating Procedure," Univ. of Colorado, NBS JILA Report
    24 (1964).

21. D. H. Hummer, _Maths. Comput._ 18, 317 (1964).

22. E. E. Whiting, _J. Quant. Spectrosc. Radiat. Transfer_, 8, 1379 (1968).

23. D. W. Posener, _Aust. J. Phys._ 12, 184 (1959).

24. H. C. Van De Hulst and J. J. M. Reesinck, _Astrophys. J._ 106, 121
    (1947).

25. R. Landenberg and F. Reiche, _Ann. Physik_, 42, 181 (1913).

26. W. M. Elsasser, "Heat Transfer by Infrared Radiation in the Atmosphere,"
    Harvard Meteor. Studies No. 6, Harvard Univ. Press, Cambridge, Mass.
    (1942).

27. R. M. Goody, "Atmospheric Radiation I: Theoretical Basis," Oxford
    Univ. Press, London and New York (1964).

28. G. N. Plass, _J. Meteorl._ 11, 163 (1954).

29. G. N. Plass, _J. Opt. Soc. Amer._ 48, 690 (1958).

30. C. L. Tien, J. Quant. Spectrosc. Radiat. Transfer 6, 893 (1966).

31. C. L. Tien, "Thermal Radiation Properties of Gases," Advances in
    Heat Transfer, Vol. V, Academic Press, New York (1968).

32. P. A. Jansson and C. L. Korb, J. Quant. Spectrosc. Radiat. Transfer 8, 1399 (1968).

33. H. Y. Yamada, J. Quant. Spectrosc. Radiat. Transfer, 8, 1463 (1968).

34. B. H. Armstrong, J. Atmos. Sci. 25, 312 (1968).

35. R. D. Cess and L. S. Wang, Int. J. Heat Mass Transfer 13, 547 (1970).

36. D. K. Edwards and S. J. Morizumi, JQSRT 10, 175 (1970).

37. S. H. Chan and C. L. Tien, JQSRT 9, 1261 (1969).

38. L. D. Kaplan, 1953 Proc. Toronto Met. Conf. (Roy. Met. Soc.), 43 (1954).

39. P. J. Wyatt, V. R. Stull, and G. N. Plass, J. Opt. Soc. Am. 52, 1209 (1962).

40. G. N. Plass, J. Opt. Soc. Am. 50, 868 (1960).

41. R. D. Cess, P. Mighdoll, and S. N. Tiwari, Intern. J. Heat Mass Transfer 10, 1521 (1967).

42. D. K. Edwards and W. A. Menard, Appl. Opt. 3, 621, 847 (1964).

43. R. M. Goody and M. J. S. Belton, Planet. Space Sci. 15, 247 (1967).

44. C. B. Ludwig, W. Malkumus, M. Griggs, and E. R. Bartle, "Monitoring of Air Pollution By Satellites (MAPS)," NASA CR-112137, prepared under Contract No. NAS1-11111 by General Dynamics Corporation for NASA's Langley Research Center, April 1972.

45. S. N. Tiwari and R. D. Cess, J. Quant. Spectrosc. Radiat. Transfer 11, 237 (1971).